applied sciences

MDPI

Article

DF Relayed Subcarrier FSO Links over Malaga Turbulence Channels with Phase Noise and Non-Zero Boresight Pointing Errors

George K. Varotsos [1], Hector E. Nistazakis [1,*], Wilfried Gappmair [2], Harilaos G. Sandalidis [3] and George S. Tombras [1]

1 Department of Electronics, Computers, Telecommunications and Control, Faculty of Physics, National and Kapodistrian University of Athens, 15784 Athens, Greece; georgevar@phys.uoa.gr (G.K.V.); gtombras@phys.uoa.gr (G.S.T.)

2 Institute of Communication Networks and Satellite Communications, Graz University of Technology, 8010 Graz, Austria; gappmair@tugraz.at

3 Department of Computer Science and Biomedical Informatics, University of Thessaly, Papasiopoulou 2-4, 35131 Lamia, Greece; sandalidis@dib.uth.gr

* Correspondence: enistaz@phys.uoa.gr; Tel.: +30-22310-66719

Received: 16 February 2018; Accepted: 13 April 2018; Published: 25 April 2018

Abstract: Subcarrier free-space optical (FSO) systems using coherent recovery techniques at the receiver have acquired growing research interest in recent times. However, their optimal performance is diminished by the non-perfect synchronization of carrier frequency and phase, which is mainly due to phase noise problems. Moreover, turbulence and pointing error effects further deteriorate the overall performance. However, relay transmission schemes can extend the coverage distance and offer substantial improvements over fading conditions. In this respect, we consider a serially relayed network using decode-and-forward relays, and investigate its performance by means of average symbol error probability and mean outage duration. Turbulence is modeled by the recently unified *M*(alaga) distribution, which constitutes a very general statistical model that accurately describes the irradiance fluctuations from weak-to-strong turbulence conditions. Additionally, the presence of non-zero boresight pointing errors due to misalignment between the transmitter–receiver pair is considered, while the effect of phase noise is specified by a Tikhonov distribution. A comparison between single line-of-sight and serially relayed FSO configurations is provided as well. Novel approximated mathematical expressions are deduced, which are proved to be accurate enough over a wide range of turbulence strengths and signal-to-noise values. Finally, proper numerical results are presented and validated by Monte Carlo simulations.

Keywords: free-space optics (FSO); multi-hop transmission; atmospheric turbulence; pointing errors; phase noise

1. Introduction

The increasing requirement for high data rates, low cost, and improved security over recent years has given rise to the employment of terrestrial free-space optics (FSO) as a potential technology for point-to-point communications. FSO systems are characterized by a plethora of prominent advantages, including, among others, unlicensed operation, small power consumption, immunity with respect to multipath dispersion, and electromagnetic interference, as well as flexibility for deployment and re-deployment due to their compactness and the rather low installation cost [1,2].

However, the propagation of optical beams is impaired by several deleterious effects that overwhelmingly emerge from the varying nature of the atmospheric medium. Absorption (mainly due to molecules of water, carbon dioxide, and ozone), aerosol scattering (mainly due to fog particles), and the dispersion of group velocity often attenuate the signal to a certain degree. Additionally, refractive index variations along the propagation path originate from the very complex atmospheric turbulence process, and result in the so-called scintillation effect, which causes rapid fluctuations in the irradiance of the optical signal at the receiver side. Furthermore, FSO links suffer from misalignment effects between transmitter and receiver terminals, leading to intensity variations in the received signals as well [2].

In the context of FSO communications, several modulation formats have been proposed and implemented, including on–off keying (OOK), pulse-position modulation (PPM), and subcarrier intensity modulation (SIM) [3]. By assigning data from different users to different subcarriers, SIM systems can achieve a higher capacity or throughput than OOK and PPM schemes with comparatively lower bandwidth than PPM. However, this comes at the cost of increased transmitter power and cross-talk [4]. On the other hand, if SIM techniques are applied, some degradation of the error performance has to be taken into consideration due to the non-perfect synchronization of the carrier frequency and phase [5]. Indeed, from a practical point of view, it is very hard to obtain an accurate estimation of the phase of the received signal [6]. This difficulty is to a large extent due to phase noise, which is a stochastic process normally described by a Tikhonov distribution [7].

The impact of turbulence, along with pointing errors and phase noise, on subcarrier phase shift keying (PSK) performance has recently attracted some attention in the open literature. Niu, Cheng and Holzman in [7] applied a phase-locked loop (PLL) for phase noise compensation over strong turbulence conditions described by a K distribution. Additionally, the bit error rate (BER) performance of a subcarrier binary PSK (BPSK) system with Tikhonov and gamma-gamma models was investigated in [6] by Djordjevic. On the other hand, the BER of subcarrier BPSK and quadrature phase shift keying (QPSK) solutions was derived by Song et al. in [3] by assuming phase effects determined by a Tikhonov distribution and weak turbulence conditions using a lognormal model. More recently, Gappamair and Nistazakis in [5] complemented the study of Song et al, [3], via a gamma-gamma turbulence model in the presence of zero boresight pointing errors and phase noise. Considering an M-ary subcarrier PSK FSO system, they derived approximate closed-form average symbol error probability (ASEP) expressions, which turned out to be accurate enough over a wide signal-to-noise ratio (SNR) range.

Regarding the distance dependency of fading impairments in FSO systems, which are induced by combined turbulence and misalignment effects, we understand that shorter hops between nodes relate to a weaker amount of fading compared to the total end-to-end link. Consequently, the use of relays in FSO systems is an effective method to extend the coverage distance and lessen the negative effects of fading [8,9]. Motivated by this fact, we thoroughly investigate the performance of a multi-hop system by means of the average symbol error performance (ASEP) and the mean outage duration (MOD) per hour. To this end, we assume the freshly launched M(alaga) distribution for turbulence description, the appearance of non-zero boresight pointing errors, subcarrier intensity modulation, and phase noise effects. We employ decode-and-forward (DF) relays, where each relay decodes the signal after detection, performs modulation, and retransmits it to the next relay or the destination. It is to be emphasized that the generic M(alaga) distribution incorporates all of the well-known models describing weak-to-strong turbulence conditions.

The remainder of the manuscript is organized as follows: Section 2 describes in brief the system and channel model. In Section 3, novel mathematical expressions related to specific performance metrics are derived. To this end, we first estimate the ASEP under the assumption of negligible phase noise effects by considering both M(alaga) turbulent and non-zero boresight misalignment fading conditions. Next, we consider the impact of phase noise on the error performance; then, we deduce an estimation of the MOD per hour. Proper numerical results validated by Monte Carlo simulations are provided in Section 4 to verify the accuracy of the extracted closed-form expressions. Finally, some concluding remarks are outlined in Section 5.

2. System and Channel Model

2.1. System Model

The FSO system under consideration consists of a laser diode transmitter, a receiver, and $N-1$ serially connected DF nodes along the propagation path, which create N individual intermediate optical links (hops). We first investigate the performance of any of these links, including a link without relays. Such a link assumes SIM with M-ary PSK signals transmitted over turbulent channels characterized by a M(alaga) distribution. It is also assumed that the M-ary PSK symbols, x, are normalized to unit magnitude, i.e., $x \in \left\{ e^{j2\pi k/M} \middle| k = 0, 1, \ldots, M-1 \right\}$, and that the received baseband signal, y, is distorted by zero mean white Gaussian noise, n, where both the in-phase and the quadrature-phase components exhibit the same variance, which is specified by σ_n^2. The contribution of the fading amplitude, which depends on the path losses, the scintillation, and the pointing error effects, is determined through the fading parameter I. Furthermore, the influence of phase noise is denoted by $\theta \in [-\pi, \pi)$. Hence, the optical signal y at the receiver input, or at any DF relay input, can be written as [5]:

$$y = e^{j\theta} I\, x + n\,. \tag{1}$$

The fading amplitude I consists of the path loss parameter I_l, the factor I_a related to the atmospheric fluctuations, and the parameter I_p, which describes the misalignment-induced fading. Thus, the fading amplitude is given by the product $I = I_l I_a I_p$. In the context of this paper, we assume without loss of generality that $I_l = 1$ [5].

2.2. Phase Noise Model

Most of the SIM FSO systems use a coherent demodulation approach, which means that the carrier phase needs to be appropriately synchronized in the receiver. In such systems, the received optical signal is first converted to an electrical signal whose phase is then tracked via a PLL. However, PLL devices are not perfect [5,6]; this is mainly because the local oscillator in the electrical demodulator unit does not generate an ideal sinusoidal waveform, which would be required for perfect synchronization. This sort of imperfection is usually denoted as a phase noise effect, and characterized by a Tikhonov distribution with a probability density function (PDF):

$$f_T(\theta) = \frac{e^{\upsilon \cos\theta}}{2\pi\, I_0(\upsilon)},\ -\pi \le \theta < \pi\,, \tag{2}$$

where $I_0(\cdot)$ denotes the zero-order modified Bessel function of the first kind (Equation (9.6.16) of Abramovitz and Stegun, [10]), and υ represents the signal-to-noise (SNR) of the phase-locked loop (PLL) used for carrier synchronization.

2.3. Atmospheric Turbulence Model

The parameter I_a follows the M(alaga) model with a PDF specified by Jurado-Navas et al. in [11]:

$$f_{I_a}(I_a) = A_{(\aleph \,\mathrm{or}\, \Re)} \sum_{(\aleph \,\mathrm{or}\, \Re)} a_{k(\aleph \,\mathrm{or}\, \Re)}\, I_a^{\frac{a+k-2}{2}} K_{a-k}\left(2\sqrt{B_{(\aleph \,\mathrm{or}\, \Re)} I_a}\right), \tag{3}$$

where the subscripts $\aleph$ or $\Re$ relate to the type of parameter b being a natural or a real number [12]. Thus, for $b \in \aleph$, the summation of Equation (3) corresponds to $\sum_{(\aleph)} [\cdot] \equiv \sum_{k=1}^{b} [\cdot]$, while the other parameters are given as:

$$\begin{aligned} A_{(\aleph)} &= \frac{2\,a^{\frac{a}{2}}\,(bc)^{b+\frac{a}{2}}}{c^{\frac{a+2}{2}}\,\Gamma(a)\,(bc+\Omega)^{b+\frac{a}{2}}}, \\ B_{(\aleph)} &= \frac{ab}{bc+\Omega}, \\ a_{k(\aleph)} &= \begin{pmatrix} b-1 \\ k-1 \end{pmatrix} \frac{(bc+\Omega)^{1-\frac{k}{2}}}{(k-1)!} \left(\frac{\Omega}{c}\right)^{k-1} \left(\frac{a}{b}\right)^{\frac{k}{2}}. \end{aligned} \tag{4}$$

On the other hand, for $b \in \Re$, the summation is specified as $\sum_{(\Re)}[\cdot] \equiv \sum_{k=1}^{\infty}[\cdot]$, while the remaining parameters are determined by:

$$\begin{aligned} A_{(\Re)} &= \frac{2\,a^{\frac{a}{2}}\,(bc)^{b}}{c^{\frac{a+2}{2}}\,\Gamma(a)\,(bc+\Omega)^{b}}, \\ B_{(\Re)} &= \frac{a}{c}, \\ a_{k(\Re)} &= \frac{(b)_{k-1}(ac)^{\frac{k}{2}}}{[(k-1)!]^2 c^{k-1}(bc+\Omega)^{k-1}}, \end{aligned} \tag{5}$$

where $(b)_k$ denotes the Pochhammer symbol (Equation (06.10.02.0001.01) of Wolfram Function site in [13]). Moreover, $K_v(\cdot)$ is the v-*th* order modified Bessel function of the second kind (Equation (8.432.2) of Gradsteyn and Ryzhik in [14]),and $\Gamma(\cdot)$ is the gamma function (Equation (8.310.1) [14]). We should recall here, according to the definition of the M(alaga) distribution, that the observed field at the receiver side is supposed to consist of three terms, i.e., the line-of-sight (LOS) component, the component coupled to LOS that is quasi-scattered forward by eddies on the propagation axis, and a scatter component that is statistically independent from the previous two terms, owing to the energy scattered to the receiver side by off-propagation axis eddies [11]. Thus, a reflects a positive parameter related to the effective number of large-scale cells characterizing the scattering process, and c equals $2b_0(1-\rho)$ [12]. The values of b_0 and ρ depend on the total scatter components, while Ω is the average optical power of the coherent contribution, which consists of LOS and scattering terms coupled to the LOS term. Specifically, the parameter ρ, where $0 \le \rho \le 1$, indicates the relationship between the two scattering components of the M(alaga) model, representing the amount of scattering power coupled to the LOS component. Meanwhile, b corresponds to the amount of fading. Table 1 indicates that the M(alaga) distribution has the concrete advantage of unifying most of the well-known turbulence models reported by Jurado-Navas et al. in [11].

Table 1. Parameter set for the generation of widely used distribution models from the unifying M(alaga) distribution model, where U_L represents the line-of-sight (LOS) component, Var[·] denotes the variance operator, and $|\cdot|$ stands for the absolute value [11].

Distribution Model	Generation
Lognormal	$\rho = 0$, Var $[\,|U_L|\,] = 0$, $c \to \infty$
Gamma	$\rho = 0$, $c = 0$
K	$\Omega = 0$ and $\rho = 0$ or $b = 1$
Gamma-Gamma	$\rho = 1$, $c = 0$, $\Omega = 1$
Exponential	$\Omega = 0$, $\rho = 0$, $a \to \infty$

2.4. Non-Zero Boresight Pointing Error Model

In practice, pointing errors are determined by boresight and jitter components. The former denotes the fixed displacement between the beam and detector center, while the latter is the random beam offset [15]. The Beckmann model is a general and realistic statistical distribution model that accurately describes the pointing mismatch by taking into account the beam width, detector size, and different jitter for elevation and horizontal displacements, as well as the effect of the non-zero boresight error; it is expressed by [16]:

$$f_R(R) = \frac{R}{2\pi\,\sigma_x\sigma_y}\int_0^{2\pi}\exp\left(-\frac{(R\cos\theta-\mu_x)^2}{2\sigma_x^2}-\frac{(R\sin\theta-\mu_y)^2}{2\sigma_y^2}\right)d\theta, \tag{6}$$

where θ is the divergence angle describing the increase of the beam radius with distance z from the transmitter, which can be approximated by $w_z = \theta\, z$ for larger values of z. Additionally, $R = \sqrt{R_x^2 + R_y^2}$ is the radial displacement, with R_x and R_y representing the deviation along the horizontal and elevation axes of the detector plane, respectively. These random variables are considered as non-zero mean Gaussian random variables, i.e., $R_x \sim N(\mu_x, \sigma_x^2)$ and $R_y \sim N(\mu_y, \sigma_y^2)$, where the parameters μ_x, μ_y denote the mean values, and σ_x, σ_y symbolize the standard deviation for the horizontal and elevation displacements, respectively [16].

The Beckmann model can be suitably approximated by a modified Rayleigh distribution as [16,17]:

$$f_R(R) = \frac{R}{\sigma_{\text{mod}}^2}\exp\left(-\frac{R^2}{2\sigma_{\text{mod}}^2}\right),\ R \geq 0, \tag{7}$$

where:

$$\sigma_{\text{mod}}^2 = \left(\frac{3\mu_x^2\sigma_x^4 + 3\mu_y^2\sigma_y^4 + \sigma_x^6 + \sigma_y^6}{2}\right)^{1/3}. \tag{8}$$

Furthermore, the PDF for the irradiance depending on pointing errors can be derived as:

$$f_{I_p}(I_p) = \frac{q^2}{(A_0\, g)^{q^2}} I_p^{q^2-1},\ 0 \leq I_p \leq A_0\, g, \tag{9}$$

with g defined by:

$$g = \exp\left(\frac{1}{q^2} - \frac{1}{2q_x^2} - \frac{1}{2q_y^2} - \frac{\mu_x^2}{2\sigma_x^2 q_x^2} - \frac{\mu_y^2}{2\sigma_y^2 q_y^2}\right) \tag{10}$$

and $q_x = w_{z,eq}/2\sigma_x$, $q_y = w_{z,eq}/2\sigma_y$, and $q = w_{z,eq}/2\sigma_{\text{mod}}$, where $w_{z,eq}$ represents the equivalent beam radius at the receiver expressed by $w_{z,eq} = w_z[\sqrt{\pi}\text{erf}(v)/(2v\, e^{-v^2})]^{1/2}$. Moreover, $v = \sqrt{\pi} r_a/(\sqrt{2} w_z)$,with r_a being the radius of the circular detection aperture, and erf$(\cdot)$ stands for the error function. In addition, $A_0 = [\text{erf}(v)]^2$ is the fraction of the collected power at the center of the receiver [18]. Note that the Beckmann distribution incorporates some classical fading models such as the Rician, Hoyt (Nakagami-q), and Rayleigh distributions as particular cases [19]. Specifically, when the boresight displacement $s = \sqrt{\mu_x^2 + \mu_y^2}$ is equal to zero, i.e., $\mu_x = \mu_y = 0$, and $\sigma_x = \sigma_y$, the Beckmann model converges to the Rayleigh distribution, which is frequently used for pointing errors with zero boresight [18].

2.5. Combined Model for Turbulence and Pointing Errors

In view of the above, the combined PDF for the normalized irradiance, I, is estimated through the following integral:

$$f_I(I) = \int f_{I|I_a}(I\big|I_a) f_{I_a}(I_a)\, dI_a\,, \tag{11}$$

where $f_{I|I_a}(I\big|I_a)$ stands for the PDF of I conditioned on I_a. This is straightforwardly obtained from Equation (9) via a procedure discussed by Varotsos et al. in [17], which yields:

$$f_{I|I_a}(I|I_a) = \frac{1}{I_a} f_{I_p}\left(\frac{I}{I_p}\right) = \frac{q^2}{(A_0\, g)^{q^2} I_a}\left(\frac{I}{I_a}\right)^{q^2-1},\ 0 \leq I \leq A_0\, g\, I_a \tag{12}$$

Substituting then Equation (3) and Equation (12) into Equation (11), we obtain:

$$f_I(I) = \frac{q^2 A_{(\aleph\,\mathrm{or}\,\Re)}}{(A_0\,g)^{q^2}} I^{q^2-1} \sum_{(\aleph\,\mathrm{or}\,\Re)} a_{k(\aleph\,\mathrm{or}\,\Re)} \int_{I/A_0\,g}^{\infty} I_a^{\frac{a+k-2q^2-2}{2}} K_{a-k}\left(2\sqrt{B_{(\aleph\,\mathrm{or}\,\Re)} I_a}\right) dI_a. \tag{13}$$

Next, by replacing the Bessel function by its Meijer-Gequivalent, which wasprovided by Adamchik and Marichev in [20], and solving the integral in Equation (11) (using equations (07.34.21.0085.01) and (07.34.16.0001.01) of Wolfram Function site in [13]), we conclude that:

$$f_I(I) = \frac{q^2 A_{(\aleph\,\mathrm{or}\,\Re)} B_{(\aleph\,\mathrm{or}\,\Re)}}{2A_0 g} \sum_{(\aleph\,\mathrm{or}\,\Re)} a_{k(\aleph\,\mathrm{or}\,\Re)} B_{(\aleph\,\mathrm{or}\,\Re)}^{-\frac{a+k}{2}} G_{1,3}^{3,0}\left(\frac{B_{(\aleph\,\mathrm{or}\,\Re)}}{A_0\,g} I \,\middle|\, \begin{matrix} q^2 \\ q^2-1,\, a-1,\, k-1 \end{matrix} \right), \tag{14}$$

where $G_{p,q}^{m,n}(\cdot)$ symbolizes the Meijer-Gfunction (Equation (07.34.02.0001.01) of Wolfram Function site in [13]).

3. Performance Analysis

3.1. Error Performance for Negligible Phase Noise

3.1.1. Exact ASEP Expression

Assuming that the phase noise is negligible and I is known to the receiver, the conditional symbol error probability (SEP) for the M-PSK schemes along with the non-zero boresight pointing errors is determined by Gappmair and Nistazakis in ([5], Equation (8.22) of Simon and Alouini in [21]):

$$p_I(I) = \frac{1}{\pi} \int_0^{\pi-\pi/M} \exp\left(-\frac{\gamma \sin^2 \frac{\pi}{M}}{\sin^2 \varphi} \right) d\varphi, \tag{15}$$

where $\gamma = I^2/2\sigma_n^2$ stands for the instantaneous SNR at the receiver. Introducing the expected SNR at the receiver as $\mu_{NZB} = E[I]_{NZB}^2/(2\sigma_n^2)$, where $E[\cdot]$ denotes expectation, we have $\gamma = \mu_{NZB} I^2/E[I]_{NZB}^2$, where the subscript NZB indicates the presence of non-zero boresight pointing errors. The expected value of amplitude fading over non-zero boresight pointing errors is then obtained as follows [17,22]:

$$A_q = E[I]_{NZB} = \int_0^\infty I\, f_I(I)\, dI = \frac{A_0\, g\, (c+\Omega)}{1+q^{-2}}, \tag{16}$$

which means that $\mu_{NZB} = A_q^2/2\sigma_n^2$. By averaging Equation (15) with respect to I, the ASEP might be expressed as:

$$p_I = \int_0^\infty p_I(I) f_I(I)\, dI = \frac{1}{\pi} \int_0^\infty \int_0^{\pi-\pi/M} \exp\left(-\mu_{NZB}\, I^2 \frac{\sin^2 \frac{\pi}{M}}{A_q^2 \sin^2 \varphi} \right) f_I(I)\, d\varphi\, dI. \tag{17}$$

Replacing in the next step the exponential term in Equation (17) with the corresponding Meijer-G function provided by Adamchik and Marichev in [20] and applying the integration rule in (Equation (07.34.21.0013.01) of Wolfram Function site in [13]), we finally obtain:

$$p_I = \frac{q^2 A_{(\aleph\,\mathrm{or}\,\Re)}}{2\pi^2} \sum_{(\aleph\,\mathrm{or}\,\Re)} 2^{a+k-3} a_{k(\aleph\,\mathrm{or}\,\Re)} B_{(\aleph\,\mathrm{or}\,\Re)}^{-\frac{a+k}{2}} \int_0^{\pi-\pi/M} G_{5,2}^{1,5}\left(\frac{16\,\mu_{NZB}(1+q^{-2})^2 \sin^2 \frac{\pi}{M}}{(c+\Omega)^2 B_{(\aleph\,\mathrm{or}\,\Re)}^2 \sin^2 \varphi} \,\middle|\, \begin{matrix} \frac{2-q^2}{2}, \frac{1-a}{2}, \frac{2-a}{2}, \frac{1-k}{2}, \frac{2-k}{2} \\ 0, \frac{-q^2}{2} \end{matrix} \right) d\varphi. \tag{18}$$

3.1.2. Approximate ASEP Expression

In order to avoid the cumbersome integration procedure in Equation (18), we proceed to an approximation. To this end, we exploit that for $M \geq 4$, the conditional SEP in Equation (15) can be approximated by [5,23]:

$$p_I(I) \cong \lambda_M \mathrm{erfc}\left(\frac{I\sqrt{\mu_{NZB}}\sin\frac{\pi}{M}}{A_q}\right), \tag{19}$$

where λ_M = 1; for BPSK schemes, the relationship still holds true provided that λ_M= 1/2. Hence, after expressing the complementary error function in Equation (19) by its Meijer-Gfunction [20] and averaging with respect to I through (Equation (07.34.21.0013.01) of Wolfram Function site in [13]), the approximated ASEP for each hop is obtained as:

$$p_I \cong \frac{\lambda_M q^2 A_{(\aleph\,\mathrm{or}\,\Re)}}{2\pi^{3/2}} \sum_{(\aleph\,\mathrm{or}\,\Re)} 2^{a+k-3} a_{k(\aleph\,\mathrm{or}\,\Re)} B_{(\aleph\,\mathrm{or}\,\Re)}^{-\frac{a+k}{2}} G_{6,3}^{2,5}\left(\frac{16\mu_{NZB}(1+q^{-2})^2\sin^2\frac{\pi}{M}}{(c+\Omega)^2 B^2_{(\aleph\,\mathrm{or}\,\Re)}} \middle| \begin{matrix} \frac{2-q^2}{2}, \frac{1-a}{2}, \frac{2-a}{2}, \frac{1-k}{2}, \frac{2-k}{2}, 1 \\ 0, \frac{1}{2}, \frac{-q^2}{2} \end{matrix}\right). \tag{20}$$

Consequently, for N individual hops connected by $(N-1)$ DF serial relays, the ASEP can be expressed as [24]:

$$\begin{aligned} p_{I,tot} &\cong \sum_{i=1}^{N}\left[p_{I,i}\prod_{j=i+1}^{N}(1-2p_{I,j})\right] \\ &= \frac{\lambda_M}{2\pi^{3/2}}\sum_{i=1}^{N}\left\{\Xi_i\,\xi_i(\mu_{i,NZB})\prod_{j=i+1}^{N}\left[1-\frac{\lambda_M}{\pi^{3/2}}\Xi_j\,\xi_j(\mu_{j,NZB})\right]\right\}, \end{aligned} \tag{21}$$

where:

$$\Xi_i = q_i^2 A_{i(\aleph\,\mathrm{or}\,\Re)} \sum_{(\aleph\,\mathrm{or}\,\Re)} 2^{a_i+k_i-3} a_{k,i\,(\aleph\,\mathrm{or}\,\Re)} B_{i(\aleph\,\mathrm{or}\,\Re)}^{-\frac{a_i+k_i}{2}} \tag{22}$$

and:

$$\xi_i(\mu_{i,NZB}) = G_{6,3}^{2,5}\left(\frac{16\,\mu_{i,NZB}(1+q_i^{-2})^2\sin^2\frac{\pi}{M}}{(c_i+\Omega_i)^2 B^2_{i\,(\aleph\,\mathrm{or}\,\Re)}} \middle| \begin{matrix} \frac{1-q_i^2}{2}, \frac{1-a_i}{2}, \frac{2-a_i}{2}, \frac{1-k_i}{2}, \frac{2-k_i}{2}, 1 \\ 0, \frac{1}{2}, \frac{-q_i^2}{2} \end{matrix}\right). \tag{23}$$

For the special case, where $p_{I,i} = p_{I,j}$, $i \neq j$, which means that $\xi_1(\mu_{1,NZB}) = \xi_2(\mu_{2,NZB}) = \ldots = \xi_i(\mu_{i,NZB}) = \xi(\mu_{NZB})$ and $\Xi_1 = \Xi_2 = \ldots = \Xi_i = \Xi$, we simply obtain:

$$p_{I,tot} \cong \frac{\lambda_M\,\Xi}{2\pi^{3/2}}\,\xi(\mu_{NZB})\sum_{i=1}^{N}\prod_{j=i+1}^{N}\left[1-\frac{\lambda_M\,\Xi}{\pi^{3/2}}\,\xi(\mu_{NZB})\right] = \frac{1}{2}\left[1-\left(1-\frac{\lambda_M\,\Xi}{\pi^{3/2}}\,\xi(\mu_{NZB})\right)^N\right]. \tag{24}$$

3.2. Error Performance with Phase Noise Effects

If we express the instantaneous loop SNR as a multiple ψ of the instantaneous SNR, i.e., $\upsilon = \psi\,\gamma$ as suggested by Song et al. in [3], then under phase noise impairments, the total angular deviation, which is denoted by $\zeta = \varphi + \theta$, where θ represents the contribution introduced by the phase noise process, follows a zero-mean Gaussian PDF with total variance [5]:

$$\sigma_\zeta^2 = \sigma_\varphi^2 + \sigma_\theta^2 = \frac{1}{2\gamma} + \frac{1}{\upsilon} = \frac{1}{2\gamma}\left(1+\frac{2}{\psi}\right). \tag{25}$$

By considering also that $\gamma = \mu_{NZB} I^2/A_q^2$, the SEP conditioned on I is obtained as [5]:

$$p_t(I) \cong 1 - \frac{1}{\sqrt{2\pi\sigma_\zeta^2}}\int_{-\pi/M}^{\pi/M} e^{-\zeta^2/(2\sigma_\zeta^2)}d\zeta = \mathrm{erfc}\left(\frac{\eta_M I\sqrt{\mu_{NZB}}}{A_q}\right), \tag{26}$$

where $\eta_M = \pi \left(M\sqrt{1+2/\psi}\right)^{-1}$ is introduced for simplification reasons.

Consequently, the corresponding ASEP is given by averaging Equation (26) with respect to the PDF of I through the following integral:

$$p_t \cong \int_0^\infty \operatorname{erfc}\left(\frac{\eta_M I \sqrt{\mu_{NZB}}}{A_q}\right) f_I(I)\, dI. \tag{27}$$

By replacing the complementary error function in Equation (27) by its Meijer-G function equivalent [20], and the PDF of I by Equation (13) as well as considering the similarity between Equations (19) and (26), the ASEP is eventually derived as:

$$p_t \cong \frac{q^2 A_{(\aleph\,\mathrm{or}\,\Re)}}{2\pi^{3/2}} \sum_{(\aleph\,\mathrm{or}\,\Re)} 2^{a+k-3} a_{k(\aleph\,\mathrm{or}\,\Re)} B_{(\aleph\,\mathrm{or}\,\Re)}^{-\frac{a+k}{2}} G_{6,3}^{2,5}\left(\frac{16\eta_M^2 \mu_{NZB}(1+q^{-2})^2}{(c+\Omega)^2 B^2_{(\aleph\,\mathrm{or}\,\Re)}} \left| \begin{matrix} \frac{2-q^2}{2}, \frac{1-a}{2}, \frac{2-a}{2}, \frac{1-k}{2}, \frac{2-k}{2}, 1 \\ 0, \frac{1}{2}, \frac{-q^2}{2} \end{matrix} \right.\right). \tag{28}$$

Similarly, the corresponding ASEP of the multi-hop FSO system under consideration is given by [24]:

$$\begin{aligned} p_{t,tot} &\cong \sum_{i=1}^{N}\left[p_{t,i} \prod_{j=i+1}^{N} (1-2p_{t,j})\right] \\ &= \frac{1}{2\pi^{3/2}} \sum_{i=1}^{N} \left\{ \Psi_i\, \psi_i(\mu_{i,NZB}) \prod_{j=i+1}^{N} \left[1 - \frac{1}{\pi^{3/2}} \Psi_j\, \psi_j(\mu_{j,NZB})\right] \right\}, \end{aligned} \tag{29}$$

where:

$$\Psi_i = q_i^2 A_{i(\aleph\,\mathrm{or}\,\Re)} \sum_{(\aleph\,\mathrm{or}\,\Re)} 2^{a_i+k_i-3} a_{k,i(\aleph\,\mathrm{or}\,\Re)} B_{i(\aleph\,\mathrm{or}\,\Re)}^{-\frac{a_i+k_i}{2}} \tag{30}$$

and:

$$\psi_i(\mu_{i,NZB}) = G_{6,3}^{2,5}\left(\frac{16\,\eta_{i,M}^2 \mu_{i,NZB}(1+q_i^{-2})^2}{(c_i+\Omega_i)^2 B^2_{i(\aleph\,\mathrm{or}\,\Re)}} \left| \begin{matrix} \frac{2-q_i^2}{2}, \frac{1-a_i}{2}, \frac{2-a_i}{2}, \frac{1-k_i}{2}, \frac{2-k_i}{2}, 1 \\ 0, \frac{1}{2}, \frac{-q_i^2}{2} \end{matrix} \right.\right). \tag{31}$$

Additionally, when $p_{t,i} = p_{t,j}$, $i \neq j$, which means that $\psi_1(\mu_{1,NZB}) = \psi_2(\mu_{2,NZB}) = \ldots = \psi_i(\mu_{i,NZB}) = \psi(\mu_{NZB})$ and $\Psi_1 = \Psi_2 = \ldots = \Psi_i = \Psi$, the mathematical expression of Equation (29) takes the following form:

$$p_{t,tot} \cong \frac{\Psi}{2\pi^{3/2}}\, \psi(\mu_{NZB}) \sum_{i=1}^{N} \prod_{j=i+1}^{N} \left[1 - \frac{\Psi}{\pi^{3/2}}\, \psi(\mu_{NZB})\right] = \frac{1}{2}\left[1 - \left(1 - \frac{\Psi}{\pi^{3/2}}\, \psi(\mu_{NZB})\right)^N\right] \tag{32}$$

Finally, by ignoring the presence of pointing errors, but taking account of the phase noise effect, it can be shown that the ASEP for the single-hop FSO configuration reduces to:

$$p_{t,o} \cong \frac{A_{(\aleph\,\mathrm{or}\,\Re)}}{2\pi^{3/2}} \sum_{(\aleph\,\mathrm{or}\,\Re)} 2^{a+k-2} a_{k(\aleph\,\mathrm{or}\,\Re)} B_{(\aleph\,\mathrm{or}\,\Re)}^{-\frac{a+k}{2}} G_{5,2}^{2,4}\left(\frac{16\,\eta_M^2 \mu_{NZB}}{B^2_{(\aleph\,\mathrm{or}\,\Re)}} \left| \begin{matrix} \frac{1-a}{2}, \frac{2-a}{2}, \frac{1-k}{2}, \frac{2-k}{2}, 1 \\ 0, \frac{1}{2} \end{matrix} \right.\right), \tag{33}$$

while for multi-hop FSO configurations, we have that:

$$\begin{aligned} p_{t,o,tot} &\cong \sum_{i=1}^{N}\left[p_{t,o,i} \prod_{j=i+1}^{N} (1-2p_{t,o,j})\right] \\ &= \frac{1}{2\pi^{3/2}} \sum_{i=1}^{N} \left\{ \Theta_i\, \vartheta_i(\mu_{i,NZB}) \prod_{j=i+1}^{N} \left[1 - \frac{1}{\pi^{3/2}} \Theta_j\, \vartheta_j(\mu_{j,NZB})\right] \right\}, \end{aligned} \tag{34}$$

where:

$$\Theta_i = A_{i(\aleph\,\mathrm{or}\,\Re)} \sum_{(\aleph\,\mathrm{or}\,\Re)} 2^{a_i+k_i-2} a_{k,i(\aleph\,\mathrm{or}\,\Re)} B_{i(\aleph\,\mathrm{or}\,\Re)}^{-\frac{a_i+k_i}{2}} \tag{35}$$

and:

$$\vartheta_i(\mu_{i,NZB}) = G_{5,2}^{2,4}\left(\frac{16\,\eta_{i,M}^2\mu_{i,NZB}}{B_{i\,(\aleph\,\mathrm{or}\,\Re)}^2}\;\middle|\;\begin{matrix}\frac{1-a_i}{2},\frac{2-a_i}{2},\frac{1-k_i}{2},\frac{2-k_i}{2},1\\ 0,\frac{1}{2}\end{matrix}\right). \tag{36}$$

For $p_{t,o,i} = p_{t,o,j}$, $i \neq j$, i.e., $\vartheta_1(\mu_{1,NZB}) = \vartheta_2(\mu_{2,NZB}) = \ldots = \vartheta_i(\mu_{i,NZB}) = \vartheta\,(\mu_{NZB})$ and $\Theta_1 = \Theta_2 = \ldots = \Theta_i = \Theta$, the mathematical expression of Equation (34) boils down to:

$$p_{t,o,tot} = \frac{\Theta}{2\pi^{3/2}}\,\vartheta(\mu_{NZB})\sum_{i=1}^{N}\prod_{j=i+1}^{N}\left[1-\frac{\Theta}{\pi^{3/2}}\,\vartheta(\mu_{NZB})\right] = \frac{1}{2}\left[1-\left(1-\frac{\Theta}{\pi^{3/2}}\,\vartheta(\mu_{NZB})\right)^N\right] \tag{37}$$

3.3. Mean Outage Duration per Hour Estimation

A significant metric for the reliability of an FSO communication system is the outage probability (OP), which represents the probability that the instantaneous electrical SNR at the receiver side, γ, falls below a critical threshold, γth, corresponding to the receiver input sensitivity limit. In such a case, the FSO system does not properly operate, and the link cannot be established. More specifically, the OP of any of the N links of the examined FSO system is estimated as [8]:

$$P_{out} = \Pr(\gamma < \gamma_{th}) = F_\gamma(\gamma_{th}), \tag{38}$$

where $\Pr(\cdot)$ denotes the probability, and $F_\gamma(\cdot)$ stands for the cumulative distribution function (CDF) of the random variable γ. By estimating the above probability as a function of the normalized irradiance I, the expression for the outage probability of Equation (38) can be transformed to the following form:

$$\Pr(\gamma < \gamma_{th}) = \Pr\left(I < A_q\sqrt{\frac{\gamma_{th}}{\mu_{NZB}}}\right) = \int_0^{A_q\sqrt{\gamma_{th}/\mu_{NZB}}} f_I(I)\,dI. \tag{39}$$

By substituting Equation (14) into Equation (39) and using Equation (07.34.21.0084.01) and Equation (07.34.21.0084.01) of Wolfram Function site in [13], we obtain:

$$P_{out} = \left(\frac{q^2 A_{(\aleph\,\mathrm{or}\,\Re)}}{2}\sum_{(\aleph\,\mathrm{or}\,\Re)} a_{k(\aleph\,\mathrm{or}\,\Re)} B_{(\aleph\,\mathrm{or}\,\Re)}^{-\frac{a+k}{2}}\right) G_{2,4}^{3,1}\left(\frac{B_{(\aleph\,\mathrm{or}\,\Re)}(c+\Omega)}{1+q^{-2}}\sqrt{\frac{\gamma_{th}}{\mu_{NZB}}}\;\middle|\;\begin{matrix}1,\ q^2+1\\ q^2,\ a,\ k,\ 0\end{matrix}\right). \tag{40}$$

Furthermore, the end-to-end OP of the FSO system is expressed as [9]:

$$\begin{aligned} P_{out,TOTAL} &= 1-\prod_{n=1}^{N}(1-P_{n,out}) \\ &= 1-\prod_{n=1}^{N}\left[1-\left(\frac{q_n^2 A_{n\,(\aleph\,\mathrm{or}\,\Re)}}{2}\sum_{(\aleph\,\mathrm{or}\,\Re)} a_{k,n(\aleph\,\mathrm{or}\,\Re)} B_{(\aleph\,\mathrm{or}\,\Re)}^{-\frac{a_n+k_n}{2}}\right) G_{2,4}^{3,1}\left(\frac{B_{n\,(\aleph\,\mathrm{or}\,\Re)}(c_n+\Omega_n)}{1+q_n^{-2}}\sqrt{\frac{\gamma_{n,th}}{\mu_{n,NZB}}}\;\middle|\;\begin{matrix}1,\ q_n^2+1\\ q_n^2,\ a_n,\ k_n,\ 0\end{matrix}\right)\right]. \end{aligned} \tag{41}$$

Then, the MOD for a specific period of time is calculated as:

$$T_{od} = P_{out,\mathrm{TOTAL}}\,T_R, \tag{42}$$

with T_R being the appropriately chosen reference time. The value of T_{od} is a significant figure of merit, because in combination with the throughput of the communication system, it relates to the percentage of information loss over T_R. Additionally, the coherence time of the atmospheric turbulence, τ_0, is in the range of milliseconds [25,26], and for T_{od}, it should be verified that $T_{od} \geq \tau_0$. For the simulation experiments conducted in the next section, we assume a reference time of one hour.

4. Numerical Results

In the analysis that follows, we employ some experimental measurements of a real-world FSO link. By properly using the analytical expressions derived in the previous section, we can numerically verify the joint influence of M(alaga) fading and non-zero boresight pointing errors on the PSK performance for both single and multi-hop FSO configurations along with or without phase noise impairments.

More specifically, we adopt the parameter values used by Yang et al. and Varotsos et al. in [15,17]. The M(alaga) turbulence values are obtained by experimental measurements performed at the University of Waseda, Japan, on 15 October 2009 [27]. The specific link has been operated at λ = 785 μm at a height of 25 m above sea level, and a receiver aperture diameter of 0.1 m. Additionally, the link length is 1 km, while the optical power used for data transmission is 11.5 dBm, with a responsivity of 0.8A/W [27]. We have to bear in mind that the strength of the atmospheric turbulence effect depends on the Rytov variance, which is defined as $\sigma_R^2 = 1.23\, C_n^2\, \kappa^{7/6} L^{11/6}$, where C_n^2 represents the index of the refraction structure parameter of the atmosphere, $\kappa = 2\pi/\lambda$ is the optical wave number, and L stands for the length of the propagation path between the transmitter and the receiver. In the context of our simulation setup, we assume that $\sigma_R^2 = 0.32$, $\sigma_R^2 = 0.52$, and $\sigma_R^2 = 1.2$ for $C_n^2 = 7.2 \times 10^{-15}\,\mathrm{m}^{-2/3}$, $C_n^2 = 1.2 \times 10^{-14}\,\mathrm{m}^{-2/3}$, and $C_n^2 = 2.8 \times 10^{-14}\,\mathrm{m}^{-2/3}$, as measured on 15 October 2009 at night, during sunrise, and near midday, respectively [27]. These experimentally measured turbulence states correspond to $(a, b, \rho) = (10, 5, 1)$, $(a, b, \rho) = (10, 5, 0.75)$, and $(a, b, \rho) = (10, 5, 0.25)$ for weak, moderate, and strong M(alaga) turbulence conditions, respectively [27]. In all of the cases presented below, the average optical power of each FSO link is normalized by $\Omega + 2b_0 = 1, \Omega = 0.5$, $b_0 = 0.25$, while the examined FSO system is assumed to employ 4-PSK, 8-PSK, or 16-PSK modulation formats. Regarding the presence of non-zero boresight pointing errors, we also assume that $(r_a,\ w_z/r_a,\ \mu_x/r_a,\ \mu_y/r_a) = (5\,\mathrm{cm}, 10, 1, 2)$, whereas the parameter q is supposed to take a value of 3.6, 2.3, or 1.1, for weak-to-strong non-zero boresight pointing error effects, and for the following combination of parameters: $(\sigma_x/r_a, \sigma_y/r_a) = (1.1, 0.9)$, $(\sigma_x/r_a, \sigma_y/r_a) = (2.1, 1.5)$, and $(\sigma_x/r_a, \sigma_y/r_a) = (4.4, 4.2)$, respectively. Under these assumptions, the performance results obtained are illustrated using lines with different styles, and they are verified by various simulation results, with b being a natural number [12], and indicated by solid dots obtained with 2×10^6 random samples.

Figure 1 illustrates the outcomes of Equations (20) and (24) as a function of the expected average electrical SNR, which is determined by μ_{NZB}, under a weak M(alaga) turbulence regime with $(a, b, \rho) = (10, 5, 1)$, and a weak amount of non-zero boresight pointing mismatch with $q = 3.6$. Different PSK formats are examined assuming single-hop (N = 1), dual-hop (N = 2), and triple-hop (N = 3) configurations. The phase noise effects are considered to be negligible, while Equation (20) is used to investigate the single-hop, and Equation (24) is used to investigate the multi-hop situation, respectively. The results depicted in Figure 1 underline the performance improvement as the average electrical SNR increases and the modulation format becomes simpler. Indeed, for higher SNR values, the impact of noise leading to the erroneous detection of symbols becomes less significant. Additionally, when focusing on higher-order PSK modulation formats, the ASEP increases. Moreover, assuming that any additional hop further increases the end-to-end total link distance of the examined FSO system through multi-hop DF relaying, Figure 1 highlights that the latter happens at the expense of raised ASEP values.

Next, by using Equation (32), the ASEP for 4-PSK multi-hop configurations is visualized in Figure 2 over a wide SNR range under weak M(alaga) turbulence, along with weak-to-strong non-zero boresight pointing errors and weak-to-moderate phase noise impairments. We observe that the ASEP increases as (i) the number of hops increases;(ii) the electrical SNR decreases; and (iii) the phase noise and non-zero boresight misalignment-induced fading effects get stronger. By comparing the results in Figures 1 and 2 (for $q = 3.6$ and 4-PSK format), we realize that the former outperforms the latter, since the emergence of phase noise brings about significant degradations. Consequently, the performance comparison between the first two figures reveals the negative-side effects of phase noise on FSO transmissions.

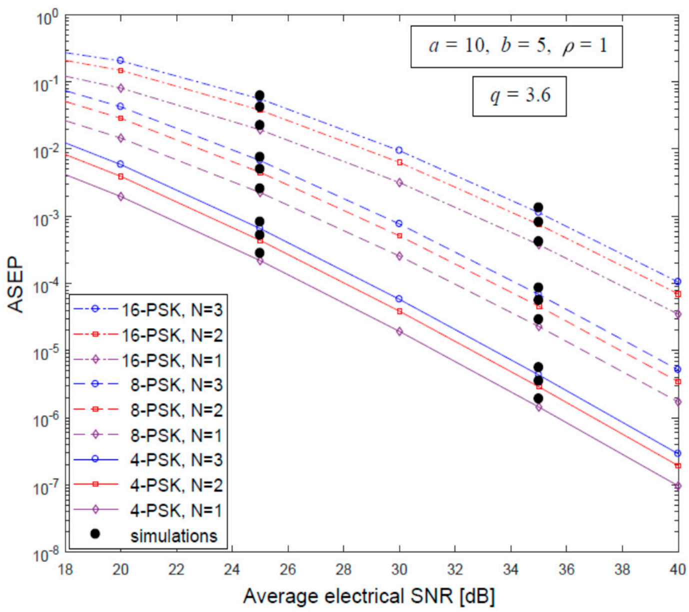

Figure 1. Average symbol error probability (ASEP) versus the average electrical signal-to-noise ratio(SNR) of single-hop or multi-hop free-space optics (FSO) configurations for weak turbulence strengths, a weak amount of non-zero boresight pointing errors, and various phase shift keying (PSK) modulation formats with negligible phase noise impairments.

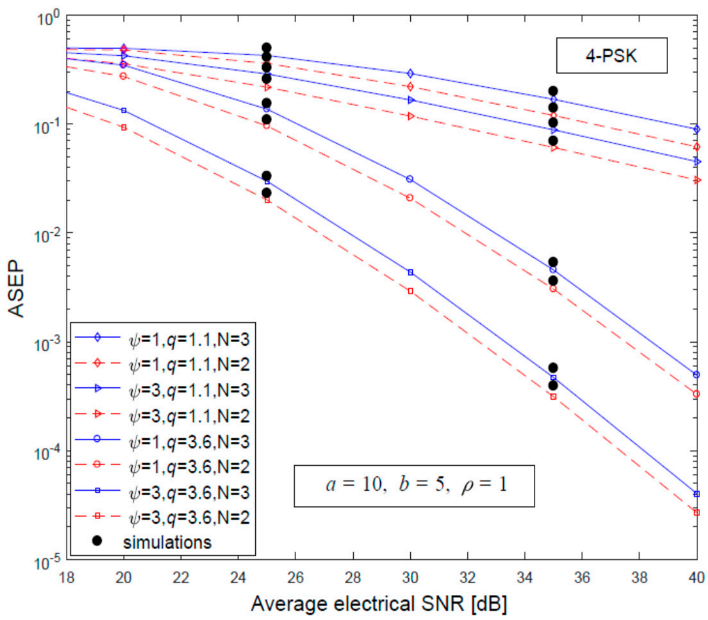

Figure 2. ASEP versus average electrical SNR of multi-hop FSO configurations for weak turbulence strengths, weak and strong amounts of non-zero boresight pointing errors, and 4-PSK modulation formats with moderate and strong phase noise impairments.

Figure 3 exemplifies the same situation as in Figure 2 through Equation (32), but now under a moderate turbulence regime governed by $\rho = 0.75$. Indeed, by assuming identical 4-PSK multi-hop configurations along with the same phase noise and non-zero boresight pointing error parameters, but over moderate, and thus stronger M(alaga) turbulence conditions, we observe that the ASEP significantly degrades. This highly demonstrates that a practical FSO system is subject to a significant ASEP increase as the atmospheric turbulence effect gets stronger.

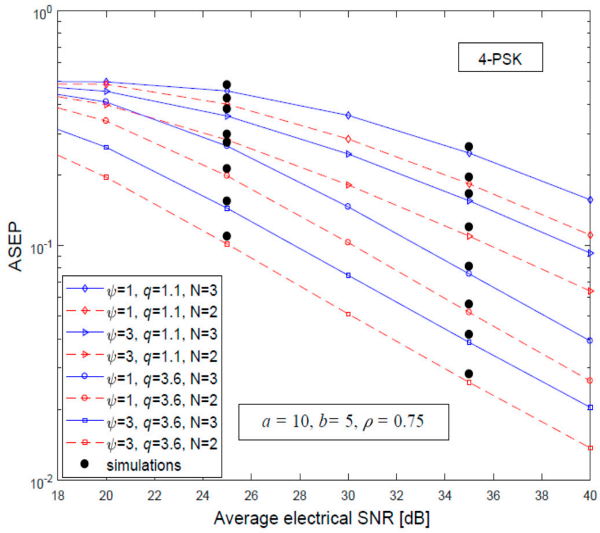

Figure 3. ASEP versus average electrical SNR of multi-hop FSO configurations for moderate turbulence strengths, weak and strong amounts of non-zero boresight pointing errors, and 4-PSK modulation formats with moderate and strong phase noise impairments.

The latter observation is also emphasized in Figure 4, where both weak and strong M(alaga) turbulent channel states are illustrated for dual-hop and triple-hop DF relaying implementations. By considering weak phase noise effects and moderate non-zero boresight misalignment, we note that for strong turbulence conditions, the use of 4-PSK signals leads to enhanced ASEP results compared with the 8-PSK scheme. Thus, in this Figure, the ASEP degradation is verified due to higher order PSK formats along with stronger turbulence-induced fading.

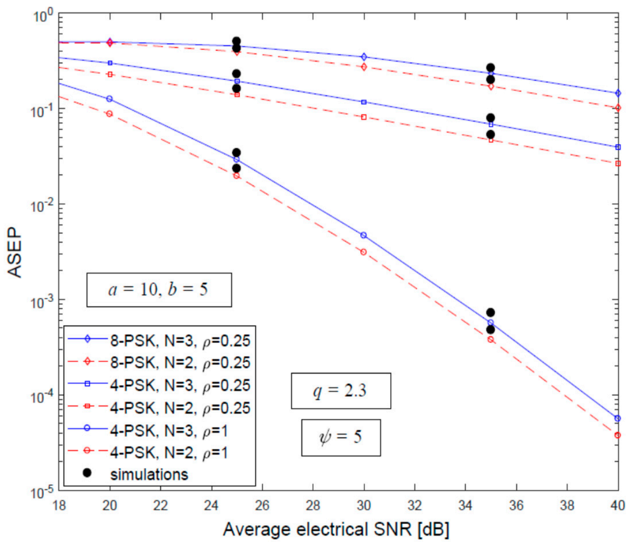

Figure 4. ASEP versus average electrical SNR of multi-hop FSO configurations for weak and strong turbulence strengths, a moderate amount of non-zero boresight pointing errors, and 4-PSK as well as 8-PSK modulation formats with weak phase noise impairments.

Finally, by using Equations (41) and (42), Figure 5 depicts the reliability by means of the MOD per hour performance metric for both single-hop and dual-hop realizations along with weak turbulence effects and weak-to-moderate non-zero boresight misalignments over a wide SNR range that is normalized by the related threshold, i.e., $\mu_{n,NZB}/\gamma_{n,th}$. We notice that both the selected modulation scheme and the phase noise process are irrelevant. Although the use of DF relays doubles the propagation distance, this leads to a severe increase of the MOD per hour values. It is also shown that the reliability increases for lower sensitivity thresholds and a weaker non-zero boresight pointing errors effect. Thus, according to the specific requirements in terms of the duration of the outage, we can make a decision—by means of an analysis based on the MOD metric—whether it is feasible to extend the FSO link length by using DF relay(s) or not.

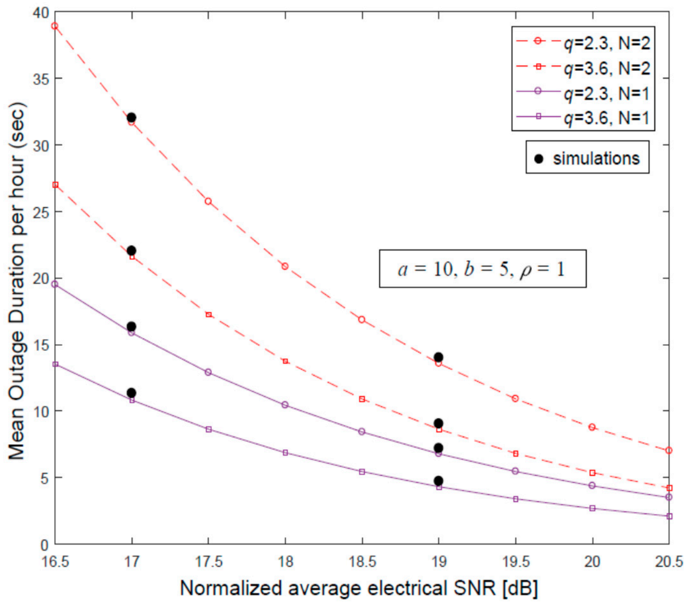

Figure 5. Mean outage duration (MOD) per hour versus normalized average electrical SNR of single-hop or dual-hop FSO configurations for weak turbulence strengths, as well as weak and moderate amounts of non-zero boresight pointing errors.

5. Conclusions

Single-hop and multi-hop FSO configurations were investigated with respect to PSK signals employing subcarrier intensity modulation. Atmospheric turbulence described by the generic M(alaga) model, along with non-zero boresight misalignment and phase noise impairments, were taken into account. Considering all of these effects, mathematical expressions for the average symbol error probability and the mean outage duration were derived. The obtained results demonstrate significant performance losses as atmospheric turbulence, non-zero boresight pointing errors, and phase noise effects are getting stronger, as more complex PSK formats are used, and as link length and the number of DF relays increase for the same total link distance. The validity of the derived mathematical expressions was properly verified through simulation results.

Author Contributions: The main idea, the theoretical part of the manuscript and the conclusions have been studied by George K. Varotsos, Hector E. Nistazakis, Wilfried Gappmair, George S. Tombras and George S. Tombras while the numerical results section has been investigated by George K. Varotsos.

Conflicts of Interest: The authors declare no conflict of interest.

References

1. Ghassemlooy, Z.; Arnon, S.; Uysal, M.; Xu, Z. Emerging optical wireless communications—Advances and challenges. *IEEE J. Sel. Areas Commun.* **2015**, *33*, 1738–1749. [CrossRef]
2. Khalighi, M.A.; Uysal, M. Survey on free space optical communication: A communication theory perspective. *IEEE Commun. Surv. Tutor.* **2014**, *16*, 2231–2258. [CrossRef]
3. Song, X.; Yang, F.; Cheng, J.; Al-Dhahir, N.; Xu, Z. Subcarrier phase-shift keying systems with phase errors in lognormal turbulence channels. *J. Lightware Technol.* **2015**, *33*, 1896–1904. [CrossRef]
4. Ghassemlooy, Z.; Popoola, W.O.; Leitgeb, E. Free-space optical communication using subcarrier modulation in gamma-gamma atmospheric turbulence. In Proceedings of the 9th International Conference on Transparent Optical Networks, Rome, Italy, 1–5 July 2007; pp. 156–160.
5. Gappmair, W.; Nistazakis, H.E. Subcarrier PSK performance in terrestrial FSO links impaired by gamma-gamma fading, pointing errors, and phase noise. *J. Lightware Technol.* **2017**, *35*, 1624–1632. [CrossRef]
6. Djordjevic, G.T. Effect of phase noise on bit error rate performance of BPSK subcarrier intensity modulated wireless optical systems—Simulation study. *Facta Univ. Ser. Autom. Control Robot.* **2014**, *12*, 189–195.
7. Niu, M.; Cheng, J.; Holzman, J.F. Error rate analysis of M-ary coherent free-space optical communication systems with K-distributed turbulence. *IEEE Trans. Commun.* **2011**, *59*, 664–668. [CrossRef]
8. Karagiannidis, G.K.; Tsiftsis, T.A.; Sandalidis, H.G. Outage probability of relayed free-space optical communications over strong turbulence channels. *Electron. Lett.* **2006**, *42*, 994–995. [CrossRef]
9. Safari, M.; Uysal, M. Relay-assisted free-space optical communication. *IEEE Trans. Wirel. Commun.* **2008**, *7*, 5441–5449. [CrossRef]
10. Abramowitz, M.; Stegun, I.A. *Handbook of Mathematical Functions*, 9th ed.; Dover Publications: New York, NY, USA, 1970.
11. Jurado-Navas, A.; Garrido-Balsells, J.M.; Paris, J.F.; Puerta-Notario, A. A unifying statistical model for atmospheric optical scintillation. In *Numerical Simulations of Physical and Engineering Processes*; Awrejcewicz, J., Ed.; Intech: Hong Kong, China, 2011; pp. 181–206.
12. Nistazakis, H.E.; Stassinakis, A.N.; Sandalidis, H.G.; Tombras, G.S. QAM and PSK OFDM RoFSO over turbulence-induced fading channels. *IEEE Photon. J.* **2015**, *7*, 1–11. [CrossRef]
13. Wolfram Function Site, Series Representation of Meijer G-Functions. Available online: http://wolfram.com (accessed on 24 April 2018).
14. Gradshteyn, I.S.; Ryzhik, I.M. *Table of Integrals, Series, and Products*, 7th ed.; Academic Press: New York, NY, USA, 2007.
15. Yang, F.; Cheng, J.; Tsiftsis, T.A. Free-space optical communication with nonzero boresight pointing errors. *IEEE Trans. Commun.* **2014**, *62*, 713–725. [CrossRef]
16. Boluda-Ruiz, R.; García-Zambrana, A.; Castillo-Vázquez, C.; Castillo-Vázquez, B. Novel approximation of misalignment fading modeled by Beckmann distribution on free-space optical links. *Opt. Express.* **2016**, *24*, 22635–22649. [CrossRef] [PubMed]
17. Varotsos, G.K.; Nistazakis, H.E.; Petkovic, M.I.; Djordjevic, G.T.; Tombras, G.S. SIMO optical wireless links with nonzero boresight pointing errors over M modeled turbulence channels. *Opt. Commun.* **2107**, *403*, 391–400. [CrossRef]
18. Farid, A.; Hranilovic, S. Outage capacity optimization for free-space optical links with pointing errors. *J. Lightware Technol.* **2007**, *25*, 1702–1710. [CrossRef]
19. Martin, J.P.P.; Jerez, J.M.R.; Lopez-Martinez, F.J. Generalized MGF of Beckmann fading with applications to wireless communications performance analysis. *IEEE Trans. Commun.* **2017**, *35*, 3933–3943. [CrossRef]
20. Adamchik, V.S.; Marichev, O.I. The algorithm for calculating integrals of hypergeometric type functions and its realization in REDUCE system. In Proceedings of the International Symposium on Symbolic and Algebraic Computation, Tokyo, Japan, 20–24 August 1990; pp. 212–224.
21. Simon, M.K.; Alouini, M.-S. *Digital Communication over Fading Channels: A Unified Approach to Performance Analysis*, 1st ed.; John Wiley: New York, NY, USA, 2000.
22. Ansari, I.S.; Yilmaz, F.; Alouini, M.-S. Performance analysis of free-space optical links over Malaga (M) turbulence channels with pointing errors. *IEEE Trans. Wirel. Commun.* **2016**, *15*, 91–102. [CrossRef]
23. Proakis, J.G. *Digital Communications*; McGraw-Hill: New York, NY, USA, 1989.

24. Nistazakis, H.E.; Stassinakis, A.N.; Muhammad, S.S.; Tombras, G.S. BER estimation for multi-hop RoFSO QAM or PSK OFDM communication systems over gamma-gamma or exponentially modeled turbulence channels. *Opt. Laser Technol.* **2014**, *64*, 106–112. [CrossRef]
25. Davis, J.; Tango, W. Measurement of the atmospheric coherence time. *Publ. Astron. Soc. Pac.* **1996**, *108*, 456–458.
26. Popoola, W.O.; Ghassemlooy, Z.; Lee, C.G.; Boucouvalas, A.C. Scintillation effect on intensity modulated laser communication systems—A laboratory demonstration. *Opt. Laser Technol.* **2010**, *42*, 682–692. [CrossRef]
27. Jurado-Navas, A.; Garrido-Balsells, J.M.; Paris, J.F.; Castillo-Vázquez, M.; Puerta-Notario, A. Impact of pointing errors on the performance of generalized atmospheric optical channels. *Opt. Express* **2012**, *20*, 12550–12562.